

Editorial Manager(tm) for Archives of Virology  
Manuscript Draft

Manuscript Number: AVIROL-D-10-00423R1

Title: The African swine fever virus lectin EP153R modulates the surface membrane expression of MHC class I antigens

Article Type: Original Article

Corresponding Author: Angel L. Carrascosa, Ph.D.

Corresponding Author's Institution:

First Author: Carolina Hurtado, Ph.D.

Order of Authors: Carolina Hurtado, Ph.D.; Maria J. Bustos, Technician; Aitor G. Granja, Ph.D.; Patricia de Leon, Ph.D.; Prado Sabina; Eduardo Lopez-Viñas, Ph.D.; Paulino Gomez-Puertas, Ph.D.; Yolanda Revilla, Ph.D.; Angel L. Carrascosa, Ph.D.

**Abstract:** We have modeled a 3D structure for the C-type lectin domain of the African swine fever virus protein EP153R, based on the structure of CD69, CD94 and Ly49A cell receptors, and thus predicting that a dimer of EP153R may establish an asymmetric interaction with one MHC-I molecule. A functional consequence of this interaction could be the modulation of MHC-I expression. By using both transfection and virus infection experiments, we here demonstrate that EP153R inhibits the MHC-I membrane expression most probably by impairing the exocytosis process, without affecting the synthesis or glycosylation of MHC antigens. Interestingly, the EP153-mediated control of MHC requires the intact configuration of the lectin domain of the viral protein, and specifically the R133 residue. Interference of EP153R gene expression during virus infection and studies with virus recombinants with the EP153R gene deleted, further support the inhibitory role of the viral lectin on the expression of MHC-I antigens.

**The African swine fever virus lectin EP153R modulates the surface membrane expression of MHC class I antigens**

Carolina Hurtado · Maria José Bustos · Aitor G. Granja · Patricia de León · Prado Sabina · Eduardo López-Viñas · Paulino Gómez-Puertas · Yolanda Revilla · Angel L. Carrascosa

C. Hurtado · M. J. Bustos · P. de León · P. Sabina · P. Gómez-Puertas · Y. Revilla · A. L. Carrascosa (✉)  
Centro de Biología Molecular “Severo Ochoa” (C.S.I.C.-U.A.M.). Consejo Superior de Investigaciones Científicas. Universidad Autónoma de Madrid, 28049 Madrid, Spain  
e-mail: [acarrascosa@cbm.uam.es](mailto:acarrascosa@cbm.uam.es)

A. G. Granja.  
Lymphocyte Interaction Lab, Cancer Research UK London Research Institute, Lincoln’s Inn Fields Laboratories, 44 Lincoln’s Inn Fields, London WC2A 3PX, United Kingdom.

E. López-Viñas.  
Biomol-Informatics SL, Parque Científico de Madrid, Campus de Cantoblanco, 28049 Madrid, Spain

## Abstract

We have modeled a 3D structure for the C-type lectin domain of the African swine fever virus protein EP153R, based on the structure of CD69, CD94 and Ly49A cell receptors, and thus predicting that a dimer of EP153R may establish an asymmetric interaction with one MHC-I molecule. A functional consequence of this interaction could be the modulation of MHC-I expression. By using both transfection and virus infection experiments, we here demonstrate that EP153R inhibits the MHC-I membrane expression most probably by impairing the exocytosis process, without affecting the synthesis or glycosylation of MHC antigens. Interestingly, the EP153-mediated control of MHC requires the intact configuration of the lectin domain of the viral protein, and specifically the R133 residue. Interference of EP153R gene expression during virus infection and studies with virus recombinants with the EP153R gene deleted, further support the inhibitory role of the viral lectin on the expression of MHC-I antigens.

## Introduction

Virus infection of susceptible organisms may trigger a cascade of mechanisms designed to minimize the cytopathogenicity and spread of the viral invasion. The induction of cytokines and activation of cytotoxic T lymphocytes (CTLs), as well as the natural killer (NK) cell response and the generation of antibodies, play a critical role in the innate and adaptative immune response of the infected host. Furthermore, the control of cell cycle and apoptosis frequently mediated by p53, have also been described as tools in the defense of cells against virus infections. Upon infection, viral proteins are processed into small peptides by the proteasome, and transported to the lumen of the endoplasmic reticulum (ER), where they associate with molecules of the class I major histocompatibility complex (MHC-I). The resulting complex then leaves the ER and is conducted, via Golgi, to the surface of the cell, where it can be recognized by receptors on CTLs and NK cells. While the interaction of MHC-I molecules with CTL receptors stimulates cytotoxic activity against the infected cells, the lytic function of NK cells is inhibited by the binding of human leukocyte antigen class I (HLA-E) to inhibitory receptors belonging to C-type lectin-like protein families that are expressed in the membrane of NK cells.

Therefore, one of the most effective and well-established defenses against the host immune response by viruses is the down-modulation of MHC-I expression [1], thus impairing the presentation of viral antigens to T lymphocytes. Moreover, as in the case of cytomegalovirus infection, the down-regulation of MHC-I expression, that should enhance the NK recognition of virus-infected cells, is counteracted by the action of several virus proteins (US2, US3, US6, US11, UL16, UL18, UL40, etc.), which interfere with different steps in the normal pathway of antigen presentation (reviewed in [2]).

The African swine fever virus (ASFV) is the sole member of the family *Asfarviridae* and of the genus *Asfivirus*, as recognized in the eight Report of the International Committee on Taxonomy of Viruses. The virus produces an important disease in domestic pigs, and can be maintained in a sylvatic cycle between wild swine and argasid ticks of the genus *Ornithodoros*. Highly lethal to subclinical disease forms have been described in the ASFV infection of both wild and domestic swine, which may depend on the contribution of different viral and host factors. Several ASFV genes are able to modulate the host defence mechanisms (A238L, A179L, A224L, EP402R, EP153R,...), interfering with cellular transcription factors or with the induction of programmed cell death after ASFV infection (reviewed in [3]). The open reading frame EP153R of ASFV encodes a non-essential protein which has been shown to be involved in the control of the apoptotic process induced in ASFV-infected cells [4]. Comparison of this sequence with data available in the literature revealed the existence of a region homologous to C-type lectins in the viral protein. Protein EP153R presents an intracellular N-terminal domain, a

1 hydrophobic segment that is probably inserted in the plasma membrane, and an extracellular region that contains  
2 the C-type lectin domain.

3  
4 Crystallographic models of several C-type lectin molecules, such as CD94, Ly49A and CD69 [5-7]  
5 allowed us to model the three-dimensional (3D) structure of the ASFV lectin in parallel with those described for  
6 the inhibitory NK cell receptors, and so consider the possible interaction between pEP153R and MHC-I  
7 molecules. Hence, the modeling of the pEP153R molecule as a dimer, points to a possible interaction with MHC-  
8 I antigens on the basis of the previously known interaction between the NK cell C-type lectin-like receptor  
9 NKG2D and its MHC-I-like ligand ULBP3. We here describe, by using swine, mouse and human cell lines  
10 ectopically expressing EP153R, a significant down-regulation of MHC-I expression. Importantly, the inhibition of  
11 MHC-I expression detected in the plasma membrane requires the intact configuration of the lectin domain of the  
12 EP153R gene, and specifically the conservation of its 133 arginine residue. Furthermore, the presence of EP153R  
13 did not affect the synthesis, maturation or degradation of the nascent MHC-I molecules, but inhibited the process  
14 of exocytosis of these molecules from the ER to the cell membrane. Finally, an increased expression of MHC-I  
15 antigens was observed when the EP153R gene was inhibited by specific siRNA transfection during ASFV  
16 infection, while the studies with ASFV recombinants with the EP153R gene deleted also revealed a higher  
17 expression of SLA-I in the plasma membrane during infection of porcine cells in the absence of EP153R  
18 transcription.

## Materials and methods

### Cells and viruses

Vero (African green monkey kidney), Raw (murine macrophages) and Jurkat (human leukemia T cell line) cells were obtained from the American Type Culture Collection. The established cell line IPAM, derived from swine alveolar macrophages [8], was obtained from Dr. M. Parkhouse, Instituto Gulbenkian de Ciencia, Portugal. Vero and COS-1 cells were grown in Dulbecco's modified eagle medium (DMEM; Gibco) supplemented with 5% fetal calf serum (FCS). IPAM, Raw and Jurkat cell cultures were grown in RPMI 1640 medium supplemented with 10% FCS. All media were supplemented with 2 mM L-glutamine, 100 U of gentamicin per ml and non-essential amino acids. Cells were grown at 37°C in 7% CO<sub>2</sub> in air saturated with water vapor. Jurkat cells were stimulated by phorbol 12-myristate 13-acetate (PMA; Sigma) at 15 ng/ml and A23187 calcium ionophore (Ion; Sigma) at 1 µM (PMA/Ion) when required.

The Vero-adapted ASFV strain BA71V and the WR strain of Vaccinia virus, were propagated and titrated by plaque assay on Vero cells as described elsewhere [9,10]. The virulent field isolates E70 and Uganda 59 of ASFV [11,12] were grown and assayed on cultures of swine macrophages [9] or in COS-1 cells as previously described [13]. The construction and characterization of the ASFV deletion mutant lacking gene EP153R ( $\Delta$ EP153R) from the Vero-adapted BA71V virus strain has been reported previously [14]. A new virus recombinant lacking the EP153R gene has been generated from the E70 ASFV isolate, by *in vivo* homologous recombination using the same deletion plasmid (p $\Delta$ EP153R) described before [14], which was designed to facilitate the replacement of a genomic DNA fragment of 333 bp covering the majority of EP153R, with the marker gene LacZ under the control of the ASFV promoter p72. The construction, selection and purification of the deletion mutant virus clones, was performed as previously described [15,14]

Virus infections were performed at 37°C: briefly, Raw or IPAM cell cultures were infected with the corresponding virus in a small volume of culture medium containing infective virus to obtain a multiplicity of infection (moi) of 3 plaque-forming units (pfu) per cell. After 1.5 h of adsorption, the non-adsorbed virus was removed and fresh culture medium added to further incubate the cultures at 37°C for the times indicated.

### EP153R-derived constructs

EP153R (whole gene or derived constructs) was subcloned into the pcDNA3.1 Myc/His mammalian expression vector (Invitrogen). Two constructs were first generated from the EP153R gene: one ("lectin C") containing the whole lectin-C domain (sequence from Trp51 to Lys153), but not the intracellular region of the molecule; and the other ("trunc lectin C") with the same domain without the last 5 amino acids in the carboxyl end of the molecule (sequence Trp51-Leu148). This deletion included the Cys151 that may be involved in a disulfide bond with Cys97 which is critical to maintaining the 3D structure of the lectin domain. The whole EP153R gene or fragments derived from the gene were PCR-amplified using oligonucleotides which included the BamHI and EcoRI restriction sites, to facilitate cloning into the pcDNA3.1 Myc/His plasmid.

The oligonucleotides used for the whole EP153R gene were:

5'-CGCGGATCCATGTATTTTAAGAAAAAATAC-3'

5'-CGCGAATTCATTATTTACCACAAATAAAT-3'

-The oligonucleotides used in the "lectin C" construct were:

5'-CGCGGATCCATGTGGGATAATTATATAAAA-3'

5'-CGCGAATTCATTACCACAAATAAAA-3'

-The oligonucleotides used in the "trunc lectin C" construct were:

5'-CGCGGATCCATGTGGGATAATTATATAAAA-3'

5'-CGCGAATTCATAATAATAAATCTGTAT-3'

We also generated two additional constructs ("R133D" and "R133K") by site-directed mutagenesis in the arg133 residue of the whole EP153R gene, by replacing it with aspartic acid or lysine in the pcDNA-EP153R plasmid (50 ng) with the following primers:

R133D:

forward (5'-CAATACGGTAATATTAGATGGTGATAATAAATATAGTC-3')

reverse (5'-ATTTATTATCACCATCTAATATTACCGTATTGTTAACCC-3');

R133K:

forward (5'-CAATACGGTAATATTTAAAGGTGATAATAAATATAGTC-3')

reverse (5'-ATTTATTATCACCATTTTATATTACCGTATTGTTAACCC-3').

The PCR reaction was performed with 2 units of Pfu enzyme DNA polymerase (Promega) by 16 cycles of denaturation at 94°C for 30 s, annealing at 55°C for 45 s, and extension at 68°C for 10 min. The constructs were digested with 10 units of Dpn1 (Promega) and transformed (3 µl) in E. coli competent cells (JM109), before being sequenced to confirm the mutagenesis.

The EP153R gene was also cloned into the pEGFP-C2 plasmid, to generate the ASFV lectin gene fused to the green fluorescent protein gene (pEGFP-EP153R). EP153R gene was PCR-amplified by using two oligonucleotides which included the Hinde III and EcoRI restriction sites, to facilitate the cloning into the pEGFP-C2 plasmid. The oligonucleotides were:

5`-CGCAAGCTTGATGTATTTTAAGAAAAATACATCGG-3`

5`-CGCGAATTCTTATTTACCACAAATAGATAATAA-3`

#### Transfections

For transient expression, cells were plated at  $1 \times 10^6$  cells per 6-cm dish, 24 h before being transfected with 2  $\mu$ g of the corresponding plasmid, using 12  $\mu$ l of Lipofectamine (2 mg/ml; Invitrogen) per dish. To generate stably expressing lines, cells were transfected as described above and incubated for 2 days before being trypsinized, and plated at 1:10 dilution in 10-cm dishes. The following day, antibiotic selection was applied (500  $\mu$ g/ml G418; Sigma) and cells were refed with the medium and fresh antibiotic every 3 days until colonies were apparent (2-3 weeks).

#### Expression of MHC-I antigens by flow cytometry

The expression of MHC-I antigens in cellular plasma membranes was analyzed by flow cytometry. Cultures of IPAM, Raw or Jurkat cells were washed with PBS-staining buffer (1% BSA, 0.01%  $\text{NaN}_3$ , 1% FCS and 5 mM EDTA in PBS) before being incubated with porcine IgG (0.2 mg/ml; Sigma-Aldrich) for 10 min at 4°C to block Fc receptors. Cells were washed again with PBS-staining and incubated for 30 min in the dark with the specific antibody to porcine SLA-I or SLA-II antigens (BL6H4, 4B7/8 and JM1E3 for SLA-I, or BL2H4 for SLA-II, monoclonal antibodies kindly provided by Dr. Diego Llanes, Universidad de Cordoba, Spain, diluted 1/10 in PBS-staining), to murine MHC-I antigens (from Serotec, diluted 1/100 in PBS-staining) or to human MHC-I antigens (supernatant of W6/32 hybridoma [16], at a concentration of 50  $\mu$ l/ $10^6$  cell) or to human ICAM-1 (PE antihuman CD54, Pharmingen, diluted 1/50). After incubation (except for the PE-labeled human ICAM antibody) in similar conditions with the secondary antibody (specific against mouse IgG, Alexa 488 from Molecular Probes, diluted 1/500), samples were washed and suspended in PBS-staining at 4°C in the dark. Propidium iodide was used to



1 exclude dead cells, by incubation of the samples with the vital dye at a concentration of 1 µg/ml for 30 min at  
2 room temperature, before analysis of the labeled populations in a FACSCalibur flow cytometer.  
3  
4

#### 5 6 Maturation and exocytosis of MHC-I antigens 7 8 9

10 The maturation of MHC-I molecules was evaluated by determining their increased resistance to Endo-H cleavage.  
11 To perform this analysis, Jurkat cells ( $20 \times 10^6$ ) pre-stimulated with PMA/Ion as indicated above, were incubated  
12 in methionine/cysteine-free DMEM supplemented with 10% FCS, for 45 min at 37°C, then pulse-labeled at 37°C  
13 for 15 min with 1000 µCi/ml [<sup>35</sup>S]methionine-cysteine (Protein Labeling Mix, Perkin Elmer) in the same medium,  
14 and chased with complete RPMI 1640 medium supplemented with 1 mM cold methionine and cysteine at 37°C for  
15 the indicated time. At different times, cells were spun down, resuspended in 50 µl of PBS, frozen in liquid  
16 nitrogen and stored at -80°C. Cells were lysed in Nonidet P-40 lysis buffer (0.5% Nonidet P-40, 50 mM Tris-HCl  
17 pH 7.5, 5 mM MgCl<sub>2</sub>) containing a mixture of protease inhibitors (complete-mini, Roche). Lysates were  
18 centrifuged at 14,000 rpm for 10 min at 4°C, pre-cleared three times for 60 min with CL-4B beads (Sigma-  
19 Aldrich) and 3 µl of normal mouse serum, and immunoprecipitated with W6/32 monoclonal antibody (0.05  
20 µg/ml) and Protein A-sepharose beads (Sigma-Aldrich). Immunoprecipitates were normalized to equal TCA-  
21 precipitable <sup>35</sup>S-labelled protein, washed three times with Nonidet P-40 washing buffer (0.5% Nonidet P-40, 50  
22 mM Tris-HCl pH 7.4, 150 mM NaCl, 5 mM EDTA) and analyzed by SDS-PAGE in 10% acrylamide gels. Endo  
23 H (New England Biolabs) was added to the immunoprecipitates according to the manufacturer's instructions.  
24 Protein bands were visualized by autoradiography and quantified after scanning by TINA 2.09e software.  
25  
26  
27  
28  
29  
30  
31  
32  
33  
34  
35  
36  
37  
38  
39  
40

41 Exocytosis of MHC-I antigens was evaluated by detecting the molecules newly incorporated into the  
42 plasma membrane. Stably-transfected Jurkat cells ( $6.5 \times 10^6$ ) pre-stimulated by PMA/Ion for 15 min as indicated  
43 above, were incubated with an excess of W6/32 monoclonal antibody (250 µg/ml) for 60 min at 4°C. Cells were  
44 washed twice with cold PBS and incubated at 37°C for different times. At each time point, cells were transferred  
45 at 4°C to stop exocytosis and the expression of new MHC-I molecules in the plasma membrane was detected by  
46 flow cytometry with W6/32 monoclonal antibody conjugated with FITC.  
47  
48  
49  
50  
51  
52  
53  
54

#### 55 Confocal microscopy 56 57 58 59 60 61 62 63 64 65

The localization of EP153R was studied by confocal microscopy. Vero cells were grown on cover slips to  $2 \times 10^5$  cells/cm<sup>2</sup> before transfection with the plasmid pEGFP-EP153R described above. Cultures were rinsed three times with PBS and fixed with cold 99.8% methanol (Merck) for 15 min at -20°C before rehydrated twice with PBS and blocked with 1% bovine serum albumin in PBS for 10 min at room temperature. The cells were then incubated with an antibody specific to either human PDI (ER resident protein, from Sigma-Aldrich), manosidase II (Golgi marker, from Chemicon) or CD63 (lysosomal marker, from DSHB), diluted 1/100 in PBS for 2 h, rinsed extensively with PBS, and then incubated with the corresponding secondary antibody (goat anti-rabbit or mouse Alexa 594; Molecular Probes, diluted 1/500 in PBS) for 1 h at room temperature in the dark. One culture was incubated with 1-2  $\mu$ M MitoTracker Red CM-H2Ros (Invitrogen) for 1h to stain mitochondria, before collected, without antibody incubation, in parallel with the rest of the cultures. Finally, the cells were rinsed successively with PBS, distilled water and ethanol, and mounted with a drop of Mowiol (Dabco) on a microslide. Visualization of the stained cultures was performed under a fluorescence Axioskop 2 plus (Zeiss) microscope coupled to a confocal Microradiance (Bio-Rad) equipment. The images were digitalized and processed with Metamorph, Lasershap 2000.

#### Silencing of viral EP153R gene by specific siRNAs

Pre-designed siRNA specific against EP153R gene was obtained from Gene Link (Ref 27-6430-05). Two siRNA duplexes were used, with the following sequences:

siRNA #1:        EP153R-113S:    5'-GAACUAAUAUGAUAAACUCUTT  
                          EP153R-113AS: 5'-AGAGUUAUCAUAAUAGUUCTT  
 siRNA#2:        EP153R-361S:    5'-CAAUCUAUGUAUUGGGUATT  
                          EP163R-361AS: 5'-UAACCCAAUACAUAAGAUUGTT

Cells were transfected with a mixture (1:1) of siRNA duplexes (60 nM) using Lipofectamine 2000 (Invitrogen) protocols, and infected, 20 to 24h after transfection, with ASFV. At different times after infection, cells were collected to analyze the SLA-I expression by flow cytometry as described above, and the EP153R mRNA transcription by RT-PCR.

#### RT-PCR analysis of mRNA expression

For these analysis, total RNA was isolated using the Trizol reagent (Invitrogen), pre-treated (1 µg) with RQ1 DNase (Promega) to eliminate ss and ds contaminant DNA and reverse-transcribed to single-stranded cDNA with Revertaid H Minus First Strand cDNA synthesis kit (Fermentas), following the manufacturer's recommendations. The DNA was PCR-amplified with Amplitaq DNA polymerase (Roche) and the following primers: for EP153R whole gene and derived constructs:  
5'-GGGATAATTATATAAAATGTTACCG (forward) and  
5'-GACTATATTTATTATCACCGTAAT (reverse)  
and for p72 gene:  
5'-CGCGGATCCATGGCATCAGGAGGAG (forward) and  
5'-CGCGAGATCTAGCTGACCATGGGCC (reverse)  
The PCRs were performed after denaturation at 94°C for 5 min, by 25 cycles of denaturation at 94°C for 30", annealing at 55°C for 30" and extension at 72°C for 30", and a last incubation at 72°C for 10 min. Amplified cDNAs were analyzed by electrophoresis on 1% agarose gels containing ethidium bromide.

#### Homology modeling procedures

The structural models for the EP153R dimer and SLA-I molecules were built using homology modeling procedures. Sequences belonging to the families of EP153R-ASFV and swine SLA-I were obtained from databases using Blast [17] with an E-value cut-off of  $10^{-5}$  and aligned using ClustalW [18]. To ensure correct gap positioning, multiple alignments were re-evaluated using TCOFFEE [19]. Sequence-to-structure alignments were performed using the threading server Phyre [20], an improved version of 3D-PSSM [21], against the SCOP database [22]. The crystallographic coordinates of human CD69 antigen dimer (Protein Data Bank entry 1E8I [7] 54% sequence similarity), human CD94 monomer (1B6E [5] 47% sequence similarity) and murine NK receptor Ly49A dimer (1QO3 [6] 37% sequence similarity) were structurally aligned using Dali [23] prior to being used as templates for the construction of the 3D model for the lectin domains of the EP153R dimer. Transmembrane domains of EP153R were modeled using the threading server Phyre [20], and selecting 2RLF structure (Influenza A M2 transmembrane domain; 47% sequence similarity) as template. The structure for the swine SLA-I molecule (UniProt/TrEMBL entry Q8MHT7\_PIG) was modeled using murine MHC -I coordinates (PDB entry 1S7U [24]) as a template (74% sequence similarity and Blast E-value  $7.7 \times 10^{-108}$ ). Structural 3D models were built using the

SWISS-MODEL server [25-27] facilities at <http://swissmodel.expasy.org//SWISS-MODEL.html>, and their structural quality was checked using the analysis programs provided by the same server (Anolea/Gromos/Verify3D) . The model for the interaction between the EP153R dimer and SLA-I, as well as for fine positioning of the amino acids in the interface of both molecules, was also constructed by homology modeling. As a template we used the co-crystal structure of the activating NK receptor, NKG2D, in a complex with the MHC-I-like molecule ULBP3 (PDB entry 1KGC [28]). Finally, both for individual structures and for the whole complex, in order to optimize geometries, release local constraints and correct possible inappropriate contacts, the modeled assemblies were energy minimized through implementation of the GROMOS 43B1 force field in the program DeepView [29], using 500 steps of steepest-descent minimization followed by 500 steps of conjugate-gradient minimization.

## Results

### Modeling of the EP153R dimer and its interaction with SLA-I

EP153R exhibits sequence similarity to swine CD69 antigen and sequence-to-structure compatibility with the lectin domain of some C-type lectin-like domains (CTLs; all of which lack the  $\text{Ca}^{2+}$  binding site involved in sugar recognition in canonical C-type lectins) related to CD69. These characteristics prompted us to generate a 3D model for the whole EP153R protein, based on the crystallographic coordinates of some CTLs available in databases, such as human CD69 [7], human CD94 [5] and murine Ly49A [6]. Structure-based alignment (Fig. 1a) showed that most of the elements present in CD69 and related proteins are also conserved in EP153R. As indicated in the figure, a non-structured N-terminal segment (residues 1-30) is followed by a predicted transmembrane alpha helix, showing amphipathic characteristics, which spans residues 30 to 49. Finally, and preceded by a 20-amino-acid-long unstructured region, the protein exhibits a high structural correspondence to the lectin domain of the aforementioned membrane antigens, with the exception of a non-structured loop present in CD69, CD94 and Ly49A which is not found in EP153R (the large gap between Val126 and Asn127 in the alignment shown in Fig. 1a). The 3D structure of the lectin domain is maintained by the presence of several disulfide bonds between Cys residues conserved in the aligned sequences. In EP153R, there are only two Cys-Cys bonds (Cys67-Cys78 and Cys97-Cys151; Fig. 1c). A third bond in the three template lectins (Cys residues aligned to EP153R Thr129 and Val142, respectively) is used in those proteins to maintain the structure of the loop that is not present in EP153R. The positions within the alignment of the Cys residues indicated above are conserved in all the proteins, with the exception of the one corresponding to Cys67 in the Ly49A sequence, which is substituted by a glycine. In this last case, the disulfide bond is established between a Cys located 9 positions downstream and only present in Ly49A. The structure of human CD94 is also maintained by a fourth additional disulfide bond between Cys59 and Cys70 which are not present in the rest of the aligned proteins. Despite these small differences, the overall structure of CD69, CD94 and Ly49A is almost identical (Fig. 1d) to the EP153R protein (Fig. 1c), with the exception of the missing loop.

The dimer structure of EP153R (Fig. 1b) was predicted on the basis of the dimer nature of the crystallized antigens used as templates, in addition to the complementary features of the helix-H3 and beta strand-E1 structural elements, involved in the dimerization surface in all members of this protein family [7,5,6]. Modeling of the transmembrane helix (H1-TM; Fig. 1e) showed a nearly amphipathic distribution of residues, with the polar

ones facing the same side of the structure. Due to the hydrophobic membrane environment, we suggest that these polar residues are arranged in a low energy conformation, thus helping dimer stability. A putative role for Cys15 and/or Cys29, both located in the cytoplasmic part of the molecule, in the stabilization of the dimer structure cannot be inferred.

A possible interaction between an MHC-I molecule (SLA-I) and the EP153R dimer was modeled (Fig. 2a) on the basis of the known structure of the interaction between the NK cell C-type lectin-like receptor NKG2D and its MHC-I-like ligand ULBP3 [28]. As shown in Fig. 2, the groove region of the predicted model for the heavy chain of swine SLA-I (based in turn on the known structure of murine MHC-I [24]) is in contact with the lectin "heads" of the dimerized EP153R structure. As in the template [28], the interaction is not symmetric, implying different surface patches for the two EP153R lectin domains (Fig. 2b-c). Interestingly, and similarly to the NKG2D-ULBP3 interaction, both surfaces exhibit reasonable complementarities in terms of electrostatic properties (Fig. 2c), mainly involving patches of polar residues. As shown in Fig. 2c, surface atoms from residues Ile87, Arg176, Ser179 and Leu184 of swine SLA-I are in contact with the area defined by residues Asn121, Arg133 and Asp135 in one EP153R monomer. In parallel, the surface patch comprising residues Glu90, Gln93, Thr94, Arg96 and Val97 of SLA-I lies on the area delineated by amino acids Asn121, Ser122, Met123, Arg133, Asp135, Asn136 and Tyr138 of the accompanying EP153R monomer.

#### EP153R down-regulates MHC-I expression both in porcine and human cells

To determine a possible effect of the viral gene EP153R in the expression of porcine SLA-I antigens, IPAM macrophage-derived cells were stably transfected with EP153R or the control pcDNA plasmid, as indicated in Materials and methods. Both cell lines, and parental non-transfected IPAM cells, were analyzed by flow cytometry to determine the expression of SLA-I and SLA-II in the plasma membrane by using specific antibodies. As shown in Fig. 3a, the parental and pcDNA-transfected cells exhibited similar levels of SLA-I expression, while a significant reduction (around 50%) was observed in IPAM cells expressing the EP153R gene. Interestingly, the expression of SLA-II antigens was similar in all the cell lines, indicating that the down-regulation detected in the plasma membrane is specific for SLA-I antigens.

We next considered of interest to extend these studies to other cells, in order to define if the EP153R gene might produce an inhibitory effect on the MHC-I expression in human cells similar to that observed in porcine cells. To this end, parent human Jurkat cells or cells stably-transfected with either EP153R or the control

pcDNA plasmid, were incubated with anti-CD54 or anti-HLA-I (W6/32) antibody, and analyzed by flow cytometry. Fig. 3b shows that the intensity of human MHC-I expression was markedly reduced in Jurkat cells transfected with EP153R, as compared to the levels obtained in the control cultures (parental cell line or transfected with the control pcDNA plasmid). The specificity of the inhibitory effect was assessed by analyzing the expression of a different cell surface component, in this case ICAM-1, a glycoprotein belonging to the immunoglobulin superfamily of adhesion molecules. The results showed that ICAM-I expression was not affected by the presence of the EP153R gene (Fig. 3b), which again supports the idea that the viral lectin specifically inhibits the expression of MHC-I antigens. The control of expression of EP153R-specific mRNA performed by RT-PCR in the stably-transfected IPAM and Jurkat cell lines showed that the virus lectin was only transcribed in cells transfected by the EP153R gene (Fig. 3c).

The inhibition of MHC-I expression in human cells requires the intact configuration of the lectin domain of the EP153R gene and, specifically, of the R133 residue.

To evaluate the importance of different regions of the ASFV lectin in the inhibition of MHC-I expression, we generated four EP153R-derived constructs as detailed in Materials and methods: two of them contained only the lectin-C domain (without the intracellular region of the molecule), either complete ("Lectin C", Fig. 4a) or with the last 5 amino acids deleted from the carboxy terminus of the molecule ("trunc Lectin C"), while the other constructs contained the whole EP153R gene with the arg133 residue replaced either by aspartic acid or lysine ("R133D" and "R133K" respectively, Fig. 4a). Transitory or stably-transfected human Jurkat cells expressing each of the constructs were stimulated with PMA/Ion for 15 min and then analyzed by flow cytometry to evaluate the expression of MHC-I in the plasma membrane. The results shown in Fig. 4b and c revealed a considerable inhibition of surface MHC-I expression in Jurkat cells transfected with either the whole gene ("EP153R") or with the complete lectin domain ("Lectin C"), while those transfected with the control pcDNA plasmid or with "trunc lectin C" exhibited a similar intensity of MHC-I antigens in the plasma membrane. These results clearly demonstrated the importance of the lectin domain conformation of EP153R for the MHC inhibitory function displayed by the viral protein. Moreover, as also shown in Fig. 4, one single substitution of the residue 133 (arginine) by aspartic ("R133D") in the whole EP153R gene resulted in MHC-I expression returning to control levels. The corresponding change from arginine to lysine ("R133K") maintained the ability of EP153R to down-regulate the expression of MHC-I in the plasma membrane. A similar experiment was performed in IPAM cells

1 stably-transfected with the above described EP153R-derived constructs, obtaining the same results (Fig. 4d) than  
2 those presented for Jurkat cells (Fig. 4b and c), and confirming that the effect of the virus lectin on the MHC-I  
3 expression can be accomplished both in transitory and stably transfections, and in different cell lines.  
4

5 Taking together these data support our model (Fig. 2), which predicts a possible interaction between the  
6 viral lectin EP153R and class I antigens, in which the R133 residue, located in the lectin “heads” of the EP153R  
7 homodimer (Fig. 2c), should play a critical role in the interaction of both EP153R subunits with the SLA-I  
8 molecule.  
9

10 EP153R impairs the exocytosis, but not the maturation, of human MHC-I antigens.  
11  
12  
13  
14  
15

16 We next explored the mechanism by which EP153R modulates MHC-I expression in the plasma membrane. To  
17 achieve this, we first analyzed the kinetics of maturation of MHC-I antigens in human Jurkat cells stably  
18 expressing EP153R by determining the resistance of these molecules to Endoglycosidase H (Endo H) treatment,  
19 which cleaves asparagine-linked mannose rich oligosaccharides but not highly processed complex  
20 oligosaccharides from glycoproteins. Proteins correctly processed through the ER and Golgi become resistant to  
21 Endo H. Cells were pulse-labeled for 15 min, chased for different times up to 6 h and then immunoprecipitated  
22 with the MHC-I-specific W6/32 antibody. One half of each sample was treated with Endo H enzyme while the  
23 other half was maintained in Endo H reaction buffer, and analyzed, after digestion, in polyacrylamide gels. As  
24 shown in Fig. 5a, the glycosidase treatment resulted in the total conversion of the immunoprecipitated proteins to  
25 a fast-migrating band (compare +/- Endo H in 0h chase, Fig. 5a). This result indicates that the entire  $\alpha$ -chain of  
26 the MHC-I molecule was accessible to the Endo H enzyme. As maturation proceeded, the intensity of the lighter  
27 band decreased (chases from 0.5 to 6 h) in favor of the slow-migrating bands. Regarding the effect of EP153R, we  
28 could not detect significant changes in the accessibility to Endo H of MHC-I antigens, nor in the rate of MHC  
29 synthesis and degradation, either in the presence or in the absence of EP153R (Fig. 5a), thus indicating that the  
30 viral lectin does not modulate these events.  
31  
32  
33  
34  
35  
36  
37  
38  
39  
40  
41  
42  
43  
44  
45  
46  
47  
48  
49

50 The process of exocytosis of human MHC-I antigens was assessed by evaluating the incorporation of  
51 new MHC-I molecules into the plasma membrane by flow cytometry. Fig. 5b shows that Jurkat-pcDNA cells  
52 increased about 6 times the expression of new MHC-I antigens in the plasma membrane, when incubated for up to  
53 60 min at 37°C after saturation with W6/32 antibody, while Jurkat-EP153R cells displayed a very low level of  
54 MHC-I expression. The differences amounted more than 10-fold, when comparing the levels between EP153R-  
55  
56  
57  
58  
59  
60  
61  
62  
63  
64  
65



and pcDNA-transfected cells at 60 min (Fig. 5b). The expected levels of MHC-I expression (with values about 3-fold higher in the absence of EP153R expression, see Fig. 3b) were obtained when incubation after saturation was extended to between 24 and 72 h (Fig. 5c). Taken together, these results clearly indicate that the viral lectin EP153R does not interfere with the synthesis and post-translational modification/degradation of the MHC-I molecules but, most probably, with their appropriate configuration or presentation into the plasma membrane.

EP153R contains an ER retrieval signal and co-localizes with ER markers.

The presence of a double lysine motif near the extreme (positions 3, 4 or 5) of the cytoplasmic portion of the molecule has been described in several transmembrane cellular and viral proteins as an ER retrieval signal, targeting them to this subcellular compartment [30]. In the case of the ASFV lectin gene EP153R, the N-terminal extreme (exposed to the cytoplasmic side) contained two lysines in positions 4 and 5 (Fig. 1a), or three lysines in positions 3, 4 and 5 assuming that the initiator methionine was absent in the mature molecule. To analyze the subcellular localization of the ASFV lectin, Vero cells were transiently transfected with the plasmid pEGFP-C2-EP153R (see Materials and methods), and analyzed by confocal microscopy after counterstaining with molecular probes specific for ER, Golgi, Lysosomes or Mitochondria. As shown in Fig. 6, the green fluorescent label of the EGFP-EP153R protein is mainly localized close to the ER marker, and not with any of the other subcellular markers used, suggesting that most of the virus lectin accumulates in the ER when ectopically expressed in transfected cells.

MHC-I expression was also reduced by the presence of EP153R during virus infection and required the integrity of the lectin domain

To determine whether the ASFV lectin was also able to modulate the MHC-I expression during the course of a virus infection, we have used macrophage-derived Raw cells transiently transfected with EP153R, as a new model (murine) to study the function of the viral protein during either ASFV or Vaccinia virus infection. Cells were infected with  $\Delta$ EP153R, a mutant virus derived from the Vero-adapted BA71V strain of ASFV which lacks the EP153R gene [14], and analyzed at different times after infection by flow cytometry, using specific antibodies against MHC-I. As shown in Fig. 7a, the basal level of MHC-I expression in the plasma membrane was similar both in mock-pcDNA and mock-EP153R transfected cells. However, MHC-I levels increased from 4 to 16 h post-

infection (hpi) in pcDNA-transfected cells (Fig. 7a, grey bars), compared to EP153R-transfected cells (solid bars) which kept basal levels of MHC-I expression both at early and late times during ASFV-ΔEP153R infection. These results indicate that the presence of EP153R impairs the expression or the accessibility of MHC-I molecules in the cell membrane.

To further demonstrate the importance of the integrity of the lectin C domain in the modulation of MHC-I expression during virus infection, cultures of stably-transfected Raw cells expressing either the whole protein ("EP153R"), the lectin-C domain ("lectin C"), the truncated lectin ("trunc lectin C") (see Fig. 4a) or the control ("pcDNA") parental plasmid, were infected with either ASFV-ΔEP153R or Vaccinia virus, at a multiplicity of infection (moi) of 3 plaque-forming units (pfu) per cell. MHC-I expression was evaluated by flow cytometry at 18 hpi. Fig. 7b shows that both ASFV and Vaccinia virus infection enhanced the levels of MHC-I expression from <60 (mean intensity in mock-infected cultures) to 90-100 in Raw-pcDNA cells. As expected, this enhancement was not observed in Raw-EP153R cells, in agreement with the results shown in Fig. 7a. Moreover, the results obtained in Raw-Lectin C cells were similar to those obtained with the complete EP153R gene (Fig. 7b), with comparable levels of MHC-I expression in either mock-infected or virus-infected cells, thus reinforcing that the lectin C domain is the region of EP153R responsible of the inhibition of MHC-I expression. The preservation of the 3D structure of the lectin domain was found again to be critical to retain the inhibitory function, since expression of the "trunc lectin C" construct yielded similar results to those obtained for control Raw-pcDNA cells (Fig. 7b).

To further corroborate the role of the viral lectin gene in ASFV infection, porcine IPAM cells were transfected with siRNA specific against EP153R (60 nM). Twenty h after siRNA transfection, cells were infected with the ASFV-Uganda 59 isolate (moi of 3 pfu per cell) and, at different times after infection, collected to analyze the effect of silencing EP153R on SLA-I expression. As shown in Fig. 7c, the level of SLA-I expression was not importantly affected by the transfection of control siRNA, both before (Mock) or after ASFV infection. However, cultures transfected with EP153 siRNA exhibited a significantly higher expression of SLA-I induced by ASFV, especially at late times during the infection cycle (16 hpi). In parallel, the inhibition of EP153R mRNA transcription was assessed by RT-PCR. The results obtained (Fig. 7d) revealed that EP153R mRNA was detected in the infected cells at 6 hpi, with similar levels in the cultures non-transfected (white bars in c) or transfected with the control siRNA (grey bars in c), while an evident decrease of transcription was found in the samples silenced with the siRNA specific for EP153R (solid bars in c), in coincidence with the higher expression of MHC-I antigens observed in these cells.

A second approach to determine the role of EP153R during virus infection took advantage of the ASFV recombinant with the viral lectin gene deleted from the E70 isolate generated in our laboratory. IPAM cells were infected with the virulent ASFV isolate E70 or its corresponding deletion mutant for EP153R gene (ED4), and analyzed at 40 hpi for SLA-I expression by flow cytometry. Three monoclonal antibodies specific for porcine SLA-I antigens were used in this experiment (Fig. 7e), revealing a higher expression of these molecules in the cultures infected with the deletion mutant, in conditions in which the EP153R gene was not transcribed (Fig. 7f).

## Discussion

We have previously described several features derived from the amino acid sequence of the ASFV protein pEP153R, and the involvement of this viral protein in the hemadsorption and apoptotic processes observed in ASFV-infected cells [14,4]. The homology of the predicted sequence of pEP153R with several C-type lectin molecules, such as CD94, Ly49A and CD69 [5-7], prompted us to build a model of the 3D structure of the viral lectin using information based on the crystallographic coordinates of these molecules in available databases. According to this information, the predicted structure of the EP153R protein comprises a cytoplasmic non-structured N-terminal segment, followed by a transmembrane region preceding the C-type lectin domain. This last domain displays a 3D structure that is maintained by the presence of several disulfide bonds between Cys residues conserved in the aligned sequences (the non-structured loop present in the other lectin molecules is absent in EP153R). The dimer nature of the crystallized antigens used as templates helped us to define a dimer structure for EP153R. This was based on the complementarity of the helix-H3 and beta strand-E1 structural elements, and on the increased stability derived from the interacting polar residues in the transmembrane helix H1-TM. Other putative disulfide bonds between neighboring Cyst residues in the monomers should help to further stabilize the dimer structure.

A possible model for the interaction between MHC-I antigens and the EP153R dimer was then generated. To do this we used the arrangement described previously for the interaction between the NK cell C-type lectin-like receptor NKG2D and its MHC-I-like ligand ULBP3 as a template [28], and predicted reasonable electrostatic complementarities and stability of the complex. This modeled interaction between the EP153R dimer and MHC class I antigens encouraged us to predict the role of the viral protein in the modulation of MHC-I expression in living cells. Two reports have established the fine structure of the Ly49A-H-2K<sup>b</sup> complex [31] and the structural basis of the recognition of HLA-E molecules by the heterodimer NKG2A/CD94 and its specific binding to the viral MHC-homologue protein UL18 from cytomegalovirus [32]. Although the geometry of the two interactions is not the same, and they are both different from that exhibited by the template [28] used in this work for the model of the EP153R-SLA-I complex, in all these cases they have been described [32] as part of a viral immunoevasion strategy.

We have used three different cellular models (porcine, murine and human) to determine the effect of the EP153R gene in the modulation of MHC-I expression. IPAM cells, derived from swine alveolar macrophages, were chosen to analyze the effect of the ASFV lectin gene in a porcine cell environment provided by an

1 established line suitable for transfection, and derived from the target cell for “in vivo” ASFV infection. In this  
2 model we detected down-regulation of the expression of SLA-I molecules in the plasma membrane of the IPAM  
3 cells in the presence of EP153R, while the expression of class II antigens was not affected by the ASFV lectin.  
4

5 To gain further insight into the role of the EP153R gene in MHC-I expression, we used human and  
6 murine cellular lines. This allowed us to define the effect of the gene in heterologous expression, in models in  
7 which the available commercial tools were of higher specificity and sensitivity (for example, more than 10  
8 antibodies specific against different subclasses of human MHC-I can be purchased from Serotec, Santa Cruz or  
9 AbNova, while only one (JM1E3) specific against porcine SLA-I antigen is available from these suppliers).  
10 Successful transfection of both Jurkat and Raw cells with different EP153R-derived constructs resulted in the  
11 generation of established cell lines expressing the corresponding protein. The use of the Jurkat cell line allowed us  
12 to confirm that the presence of EP153R in stably-transfected cells also specifically reduced the expression of  
13 human MHC-I in the plasma membrane, since another cell surface molecule like ICAM-1 was not affected by the  
14 expression of the viral gene. Moreover, the expression of those antigens also decreased in the presence of either  
15 the whole gene (“EP153R”) or the EP153R C-type lectin domain (“Lectin C”), while the “trunc Lectin C”, that  
16 contains a deletion in the C-terminal sequence of the Lectin C, did not modulate the MHC-I expression in Jurkat  
17 cells stimulated with PMA/Ion. This was probably because of the large conformational changes induced in the  
18 lectin C domain by the deletion of the E6 region (F149 to K153, including the residue C151, a cysteine which may  
19 be involved in a disulfide bond with C97) of the EP153R molecule. The use of two EP153R-derived constructs  
20 with single substitutions of residue R133 for equivalent (K) or antagonistic (D) amino acids in terms of  
21 electrostatic charge, lends significant support to the predicted model of the interaction of EP153R with the MHC-I  
22 antigens: the down-modulation of MHC-I expression in the plasma membrane by the viral lectin was prevented by  
23 a single change from R to D in residue 133. It is interesting to note that this is a highly-conserved residue among  
24 many ASFV isolates [33], and we anticipated that this position, postulated in the lectin “heads” of the EP153R  
25 dimerized structure, was critically involved in the electrostatic complementarity predicted to be important in the  
26 interaction of both subunits of the EP153R homodimer with the groove region of the heavy chain of the SLA-I  
27 molecule.  
28

29 Regarding the murine cellular model, the level of MHC-I expression in Raw cells was not affected by the  
30 transfection of the EP153R gene. However, stably-transfected Raw macrophages showed an increased level of  
31 MHC-I expression after infection with either ASFV  $\Delta$ EP153R mutant virus or Vaccinia virus, which was  
32 prevented by the expression of either the whole EP153R gene or the “Lectin-C” construct. In contrast, the deletion  
33

of the sequence F149-K153 from the E6 region of EP153R, resulted in a construct (“trunc Lectin C”) that, as in the case of Jurkat cells, did not modulate the expression of MHC-I when transfected in Raw cells. This suggests that the preservation of the 3D structure of the lectin domain is critical to establishing the appropriate interaction between EP153R and the MHC-I molecule, and that it should be also involved in the process of virus infection.

In order to analyze the role of the EP153R gene during ASFV infection, we used two approaches, interference with siRNA and infection with virus deletion mutants. In the first approach, IPAM cells, a line of porcine macrophages that allow infection with several virulent and attenuated ASFV isolates, were infected with a virulent (Uganda 59) isolate after silencing the EP153R gene transcription with specific siRNA. The work presented in this paper indicates that a partial silencing of the EP153R gene transcription results in a moderate increase of the levels of SLA-I expression on the plasma membrane of ASFV-infected IPAM cells, thus indicating that the ASFV lectin also modulates the MHC-I expression in *in vivo* infections. For the second approach, we used an ASFV recombinant generated in our laboratory from the E70 isolate of ASFV with the EP153R gene inactivated (ED4), to infect IPAM porcine cells. We did not use in this case the BA71V isolate and its EP153R-deletion mutant (DEP), since they produce a very limited infection in IPAM cell cultures (unpublished observations). Our results revealed that the expression of SLA-I antigens in the plasma membrane was reduced in cells infected with the parental E70 strain as compared with those infected with the corresponding EP153R-deletion mutant ED4. The effect of the ASFV EP153R lectin gene was, however, less remarkable when analyzed during ASFV infection of porcine cells than in heterologous expression in EP153R-transfected cell lines. Differences in the expression levels of the viral lectin gene in each system, and/or in the specificity/sensitivity of the available antibodies to recognize the particular subclass of SLA-I involved in the interaction with EP153R, might account for these divergences.

Regarding the mechanism by which the expression of MHC-I was reduced in the presence of EP153R, we studied the possibility of an impairment in the process of maturation and exocytosis of the MHC-I molecules in the human model. Our results establish that the synthesis and glycosylation of MHC-I molecules proceeded normally, while the exocytosis of mature molecules in the plasma membrane was severely affected in Jurkat cells transfected with the EP153R gene, as compared with control pcDNA-transfected cultures. As MHC-I synthesis or degradation was not affected by the expression of EP153R, we propose that the low levels of surface MHC-I antigens observed in the presence of the viral protein might be a consequence of the misfolding or retention of MHC-I molecules in the Golgi or ER compartments. Another possibility is that the MHC-I molecules emerging in the plasma membrane are not recognized by the specific antibodies when they are associated to the viral protein

EP153R. It is also tempting to suggest a mechanism for the ASFV lectin similar to that described for adenovirus E19 protein [1], whose ability to interact with murine and human MHC-I molecules results in their retention in the ER mediated by an ER retention motif. In fact, the analysis of the sequence of the EP153R gene revealed the presence of a similar motif, with three lysines in positions 3, 4 and 5 in the cytoplasmic end of the molecule, which might direct the protein to this subcellular compartment, as described for several transmembrane cellular and viral proteins [30]. The colocalization of the EP153R protein fused to a GFP tag with ER markers in transfected Vero cells by confocal microscopy, also supported the possibility that the ASFV lectin can display a similar location to that of other viral (adeno E19) and cellular (calnexin and calreticulin) lectins, known to interact with the heavy chain of the MHC-I molecules before its association to  $\beta$ 2-microglobulin in the ER. However, further experiments are needed to explain the effective down-regulation of MHC-I antigens obtained in transfections with the “Lectin C” construct, in which the intracellular amino terminal region of EP153R was eliminated: interestingly, the absence of the ER retention signal in this construct indicated that the dilysine motif was not needed for the reduction of the MHC-I expression on the cell surface. Nevertheless, it is not excluded that the interaction EP153R - MHC-I must occur in the ER, since other single-pass transmembrane proteins in the ER, like tapasin or tyrosinase, have been shown to maintain their localization to the ER in constructs lacking the transmembrane domain and the cytoplasmic tail (which includes the ER retrieval motif) [34,35]. Alternative mechanisms for affecting MHC-I expression, such as the induction of misfolding (with impaired recognition by the specific antibodies) or the inhibition of peptide loading described for truncated versions of adenovirus E19 protein without its ER retention signal [36], could also be exploited by the ASFV lectin.

The absence of a vaccine available for ASF is a main problem for the control of the disease. However, protective immunity against homologous virus has been described in pigs surviving viral infection [37], most probably involving both humoral and cellular immunity. Although ASFV neutralizing antibodies directed against virus proteins have been reported, they are not sufficient for protection, enforcing CTLs and NK cells to have a role in the protective immune response to ASFV infection (reviewed in [3]). An efficient cellular response could be related with the persistent and non-lethal disease observed in the wild hosts and in the attenuated forms also detected in domestic pigs. Besides, a reduced expression of the MHC-I antigens in the plasma membrane of infected cell may produce both an anomalous presentation of the viral peptides to CTLs and changes in the NK cell response, suggesting that the deletion of the ASFV EP153R gene may result in a more attenuated virus, which must induce a more efficient cellular immune response.

1 In conclusion, in this report we have demonstrated a role for the ASFV lectin pEP153R in the modulation  
2 of MHC-I expression in the cell membrane. This is probably mediated by the retention of correctly glycosylated  
3 MHC-I molecules in subcellular compartments and provides a new mechanism for ASFV evasion of host antiviral  
4 responses.  
5  
6  
7  
8  
9

## 10 **Acknowledgements**

11 We are grateful to Begoña Galocha for experimental help and discussions. We also thank Biomol-Informatics SL  
12 (www.biomol-informatics.com) for bioinformatics consulting. This work was supported by grants from the  
13 Spanish Ministerio de Ciencia y Tecnología (BFU2007-63110/BMC), from the European Community's Seventh  
14 Framework Programme (FP7/2007-2013) under grant agreement KBBE- 211691- ASFRISK and from  
15 Laboratorios del Dr. Esteve, SA, and also by institutional grants from the Fundación Ramón Areces and Banco  
16 Santander Central Hispano. C.H. and A.G.G. also acknowledge financial support from the Centro de Investigación  
17 en Sanidad Animal (CISA).  
18  
19  
20  
21  
22  
23  
24  
25  
26  
27  
28  
29  
30  
31  
32  
33  
34  
35  
36  
37  
38  
39  
40  
41  
42  
43  
44  
45  
46  
47  
48  
49  
50  
51  
52  
53  
54  
55  
56  
57  
58  
59  
60  
61  
62  
63  
64  
65



## References

1. Tortorella D, Gewurz BE, Furman MH, Schust DJ, Ploegh HL (2000) Viral subversion of the immune system. *Annu Rev Immunol* 18:861-926
2. Lin A, Xu H, Yan W (2007) Modulation of hla expression in human cytomegalovirus immune evasion. *Cell Mol Immunol* 4 (2):91-98
3. Tulman ER, Delhon GA, Ku BK, Rock DL (2009) African swine fever virus. *Curr Top Microbiol Immunol* 328:43-87
4. Hurtado C, Granja AG, Bustos MJ, Nogal ML, Gonzalez de Buitrago G, de Yebenes VG, Salas ML, Revilla Y, Carrascosa AL (2004) The c-type lectin homologue gene (ep153r) of african swine fever virus inhibits apoptosis both in virus infection and in heterologous expression. *Virology* 326 (1):160-170
5. Boyington JC, Riaz AN, Patamawenu A, Coligan JE, Brooks AG, Sun PD (1999) Structure of cd94 reveals a novel c-type lectin fold: Implications for the nk cell-associated cd94/nkg2 receptors. *Immunity* 10 (1):75-82
6. Tormo J, Natarajan K, Margulies DH, Mariuzza RA (1999) Crystal structure of a lectin-like natural killer cell receptor bound to its mhc class i ligand. *Nature* 402 (6762):623-631
7. Llera AS, Viedma F, Sanchez-Madrid F, Tormo J (2001) Crystal structure of the c-type lectin-like domain from the human hematopoietic cell receptor cd69. *J Biol Chem* 276 (10):7312-7319
8. Weingartl HM, Sabara M, Pasick J, van Moorlehem E, Babiuk L (2002) Continuous porcine cell lines developed from alveolar macrophages: Partial characterization and virus susceptibility. *J Virol Methods* 104 (2):203-216
9. Carrascosa AL, Santaren JF, Vinuela E (1982) Production and titration of african swine fever virus in porcine alveolar macrophages. *J Virol Methods* 3 (6):303-310
10. Enjuanes L, Carrascosa AL, Moreno MA, Vinuela E (1976) Titration of african swine fever (asf) virus. *J Gen Virol* 32 (3):471-477
11. Garcia-Barreno B, Sanz A, Nogal ML, Vinuela E, Enjuanes L (1986) Monoclonal antibodies of african swine fever virus: Antigenic differences among field virus isolates and viruses passaged in cell culture. *J Virol* 58 (2):385-392
12. Salguero FJ, Gil S, Revilla Y, Gallardo C, Arias M, Martins C (2008) Cytokine mrna expression and pathological findings in pigs inoculated with african swine fever virus (e-70) deleted on a238l. *Vet Immunol Immunopathol* 124 (1-2):107-119
13. Hurtado C, Bustos MJ, Carrascosa AL (2010) The use of cos-1 cells for studies of field and laboratory african swine fever virus samples. *J Virol Methods* 164 (1-2):131-134
14. Galindo I, Almazán F, Bustos MJ, Viñuela E, Carrascosa AL (2000) African swine fever virus ep153r open reading frame encodes a glycoprotein involved in the hemadsorption of infected cells. *Virology* 266 (2):340-351
15. Rodriguez JM, Almazan F, Vinuela E, Rodriguez JF (1992) Genetic manipulation of african swine fever virus: Construction of recombinant viruses expressing the beta-galactosidase gene. *Virology* 188 (1):67-76
16. Barnstable CJ, Bodmer WF, Brown G, Galfre G, Milstein C, Williams AF, Ziegler A (1978) Production of monoclonal antibodies to group a erythrocytes, hla and other human cell surface antigens-new tools for genetic analysis. *Cell* 14 (1):9-20
17. Altschul SF, Gish W, Miller W, Myers EW, Lipman DJ (1990) Basic local alignment search tool. *J Mol Biol* 215 (3):403-410
18. Thompson JD, Higgins DG, Gibson TJ (1994) Clustal w: Improving the sensitivity of progressive multiple sequence alignment through sequence weighting, position-specific gap penalties and weight matrix choice. *Nucleic Acids Res* 22 (22):4673-4680
19. Notredame C, Higgins DG, Heringa J (2000) T-coffee: A novel method for fast and accurate multiple sequence alignment. *J Mol Biol* 302 (1):205-217
20. Kelley LA, Sternberg MJ (2009) Protein structure prediction on the web: A case study using the phyre server. *Nat Protoc* 4 (3):363-371
21. Kelley LA, MacCallum RM, Sternberg MJ (2000) Enhanced genome annotation using structural profiles in the program 3d-pssm. *J Mol Biol* 299 (2):499-520
22. Andreeva A, Howorth D, Brenner SE, Hubbard TJ, Chothia C, Murzin AG (2004) Scop database in 2004: Refinements integrate structure and sequence family data. *Nucleic Acids Res* 32 (Database issue):D226-229
23. Holm L, Park J (2000) Dalilite workbench for protein structure comparison. *Bioinformatics* 16 (6):566-567

24. Velloso LM, Michaelsson J, Ljunggren HG, Schneider G, Achour A (2004) Determination of structural principles underlying three different modes of lymphocytic choriomeningitis virus escape from ctl recognition. *J Immunol* 172 (9):5504-5511
25. Guex N, Diemand A, Peitsch MC (1999) Protein modelling for all. *Trends Biochem Sci* 24 (9):364-367
26. Peitsch MC (1996) Promod and swiss-model: Internet-based tools for automated comparative protein modelling. *Biochem Soc Trans* 24 (1):274-279
27. Schwede T, Kopp J, Guex N, Peitsch MC (2003) Swiss-model: An automated protein homology-modeling server. *Nucleic Acids Res* 31 (13):3381-3385
28. Radaev S, Rostro B, Brooks AG, Colonna M, Sun PD (2001) Conformational plasticity revealed by the cocrystal structure of nkg2d and its class i mhc-like ligand ulbp3. *Immunity* 15 (6):1039-1049
29. Guex N, Peitsch MC (1997) Swiss-model and the swiss-pdbviewer: An environment for comparative protein modeling. *Electrophoresis* 18 (15):2714-2723
30. Jackson MR, Nilsson T, Peterson PA (1990) Identification of a consensus motif for retention of transmembrane proteins in the endoplasmic reticulum. *Embo J* 9 (10):3153-3162
31. Deng L, Cho S, Malchiodi EL, Kerzic MC, Dam J, Mariuzza RA (2008) Molecular architecture of the major histocompatibility complex class i-binding site of ly49 natural killer cell receptors. *J Biol Chem* 283 (24):16840-16849
32. Kaiser BK, Pizarro JC, Kerns J, Strong RK (2008) Structural basis for nkg2a/cd94 recognition of hla-e. *Proc Natl Acad Sci U S A* 105 (18):6696-6701
33. Neilan JG, Borca MV, Lu Z, Kutish GF, Kleiboeker SB, Carrillo C, Zsak L, Rock DL (1999) An african swine fever virus orf with similarity to c-type lectins is non-essential for growth in swine macrophages in vitro and for virus virulence in domestic swine. *J Gen Virol* 80 (Pt 10):2693-2697
34. Everett MW, Edidin M (2007) Tapasin increases efficiency of mhc i assembly in the endoplasmic reticulum but does not affect mhc i stability at the cell surface. *J Immunol* 179 (11):7646-7652
35. Popescu CI, Paduraru C, Dwek RA, Petrescu SM (2005) Soluble tyrosinase is an endoplasmic reticulum (er)-associated degradation substrate retained in the er by calreticulin and bip/grp78 and not calnexin. *J Biol Chem* 280 (14):13833-13840
36. Bennett EM, Bennink JR, Yewdell JW, Brodsky FM (1999) Cutting edge: Adenovirus e19 has two mechanisms for affecting class i mhc expression. *J Immunol* 162 (9):5049-5052
37. Ruiz Gonzalvo F, Carnero ME, Caballero C, Martinez J (1986) Inhibition of african swine fever infection in the presence of immune sera in vivo and in vitro. *Am J Vet Res* 47 (6):1249-1252

## Figure legends

**Fig. 1.** Structural model for the EP153R dimer. **(a)** Structure-based alignment of proteins used as template for dimerized lectin domain of EP153R: human CD69, human CD94 and murine Ly49A antigens (PDB entries 1E81, 1B6E and 1QO3 respectively). Sequence of swine CD69 has been included to illustrate the similarity between EP153R and CD69 antigens. Location of predicted secondary structure elements of EP153R model (TM: transmembrane, H: alpha-helix and E: beta-strand) as well as the two Cys-Cys bonds (open and black circles respectively) are also indicated. Dotted lines indicates location of coil elements whose structure has been modeled in absence of suitable templates. **(b)** Surface, colored by charge, and ribbon-plot representation of the relative position of the two molecules of EP153R in the dimerized complex. Situation of secondary structure elements is indicated. Note the absence of electrostatic charge on the surface corresponding to the hydrophobic transmembrane helix (H1-TM). **(c)** Detail of the lectin domain (residues 64 to 153) of the EP153R model. Cys67-Cys78 and Cys97-Cys151 disulfide bond residues are depicted. **(d)** Structural alignment of CD69 (dark blue), CD94 (light blue) and Ly49A (green) lectin domains, showing the similarity among them and to the modeled EP153R lectin structure (red). Location of extra loop not present in EP153R is indicated (red circle). **(e)** Detail of the modeled transmembrane segment of EP153R. Side chains of polar residues from both helices are arranged towards the inner face of the dimer (green spheres) while the hydrophobic amino acids (yellow) are oriented to the membrane environment. Plots were generated using PyMOL (DeLano Scientific, San Carlos, CA)

**Fig. 2.** Structural model for EP153R-SLA I interaction. **(a)** Ribbon-plot representation of the relative position of the two proteins. Groove domain -yellow/orange- of the SLA-I heavy chain model comes into contact with the lectin domains (blue and green) of the EP153R dimer. **(b)** Detail of the interaction area, illustrating the asymmetric contribution of the two lectin domains of the two EP153R monomers. Also indicated is the position of helix-H3 and beta strand-E1, whose residues putatively help maintain the stability of the EP153R dimer. **(c)** Diagram indicating the surface complementarity of the interacting molecules. Bottom panel: position of residues in SLA-I and EP153R molecules predicted to be involved in protein contact.

**Fig. 3.** Modulation of MHC-I expression by EP153R-derived constructs. **(a)** Inhibition of porcine SLA-I and SLA-II expression by EP153R. IPAM cell cultures stably-transfected, or not, with pcDNA or EP153R, were

incubated with specific antibodies against porcine SLA-I or SLA-II antigens (BL6H4 or BL2H4, respectively), to analyze its expression in the plasma membrane by flow cytometry. The percentage of antigen expression is shown (mean  $\pm$  S.D. in duplicate samples), taking the value in parental IPAM cells as 100%. (b) Inhibition of human MHC-I expression by EP153R. Cultures of Jurkat cells either parental (Jurkat) or stably-transfected with pcDNA (JpcDNA) or EP153R (JEP153R), were incubated with antibody specific against human MHC-I (W6/32) or ICAM-I (CD54), to detect the expression of these molecules in the plasma membrane by flow cytometry. The intensity of the antigen expression is shown (mean  $\pm$  S.D. in duplicate samples), representing the results obtained in two independent experiment. (c) The mRNA transcription specific for EP153R gene was assayed in stably-transfected Jurkat and IPAM cell lines by RT-PCR.

**Fig. 4. (a)** EP153R-derived constructs. Representation of the constructs generated from EP153R as indicated in Materials and methods. The position of secondary structure elements is indicated (TM: transmembrane, H: alpha-helix and E: beta-strand) and numbered successively, as shown in Fig. 1a. “EP153R”: whole gene; “Lectin C”: sequence from Trp51 to Lys153; “trunc Lectin C”: sequence from Trp51 to Leu148; “R133D”: whole EP153R gene with the mutation arg133asp; “R133K”: whole EP153R gene with the mutation arg133lysin. (b, c) Effect of different EP153R-derived constructs on human MHC-I expression. Jurkat cells, transitory (b) or stably (c) transfected with pcDNA or different constructions derived from EP153R (as described in a) were stimulated with PMA/Ion for 15 min, and then incubated with human MHC-I (W6/32) antibody before flow cytometry analysis. (d) Effect of different EP153R-derived constructs on porcine SLA-I expression. IPAM cells, stably-transfected with the EP153R-derived constructs, were incubated with porcine SLA-I (BL6H4) antibody to detect the expression of these molecules in the plasma membrane by flow cytometry. The intensity of the antigen expression in the plasma membrane is shown (mean  $\pm$  S.D. in duplicate samples). (e) The mRNA transcription specific for EP153R gene was assayed in Jurkat stably-transfected cell lines by RT-PCR.

**Fig. 5. (a)** Maturation of human MHC-I molecules. Jurkat cells stably-transfected with pcDNA or EP153R, were pre-stimulated with PMA/Ion, pulse-labeled for 15 min with [<sup>35</sup>S]methionine-cysteine and chased at 0, 0.5, 2, 4 and 6 h after labeling. Cells were then lysed, immunoprecipitated with human MHC-I (W6/32) antibody and treated either with Endo H enzyme (+) or with buffer alone (-). Proteins were separated by SDS-PAGE and

visualized by autoradiography. The corresponding positions of MHC-I molecules either resistant (Endo H<sub>R</sub>) or sensitive (Endo H<sub>S</sub>) to Endo H enzyme are indicated. (b, c) Exocytosis of human MHC-I molecules in the presence of EP153R. Jurkat cells stably-transfected with pcDNA or EP153R were stimulated with PMA/Ion for 15 min, and then incubated with an excess of W6/32 monoclonal antibody for 60 min at 4°C. After saturation, cells were washed with PBS and further incubated at 37°C for the times indicated in the figures (b, short-term and c, long-term) before being cooled again to 4°C. Samples were then incubated with W6/32 monoclonal antibody conjugated to FITC to detect the expression of new MHC-I molecules by flow cytometry. The intensity of the antigen expression in the plasma membrane is shown (mean ± S.D. in duplicate samples), representing the results obtained in three independent experiments. The control of EP153R-specific mRNA transcription by RT-PCR in stably-transfected Jurkat cell lines is shown in Fig. 3c.

**Fig. 6.** Expression of EGFP-EP153R protein. Vero cells transiently transfected with the ASFV EP153R gene fused to EGFP, were labeled with MitoTracker to stain mitochondria or incubated with antibodies specific for cellular ER, Golgi or Lysosome as indicated under Materials and methods, and examined by confocal microscopy.

**Fig. 7.** Modulation of MHC-I expression by EP153R gene in virus infections. (a) Inhibition of murine MHC-I expression by EP153R. Cultures of Raw cells transiently transfected with pcDNA or EP153R were mock-infected or infected with ASFV-ΔEP153R and incubated, at the indicated times after infection (hpi), with antibody specific for murine MHC-I antigens, to analyze the expression of these molecules in the plasma membrane by flow cytometry (mean ± S.D. in duplicate samples). (b) Effect of different constructs derived from EP153R on murine MHC-I expression. Raw cells stably transfected with pcDNA or different EP153R-derived constructs (EP153R, Lectin C or trunc Lectin C), were mock-infected or infected with ASFV-ΔEP153R or Vaccinia virus as described in Materials and methods. Cells collected at 18 hpi were incubated with murine MHC-I antibody to detect the MHC-I expression in the plasma membrane by flow cytometry. The intensity of the antigen expression is shown (mean ± S.D. in duplicate samples). (c) Modulation of SLA-I expression by siRNA specific for EP153R. IPAM cells were transfected or not with control (irrelevant) or EP153R-specific siRNA (60 nM), and infected 20 h after transfection with the Uganda 59 isolate of ASFV. At the times indicated duplicate samples were collected to

determine the expression of SLA-I (BL6H4) in the plasma membrane by flow cytometry (c) and the EP153R mRNA transcription by RT-PCR (d). The intensity of the antigen expression is shown (mean  $\pm$  S.D.). Results representative of several experiments (more than six), including infections with other virulent ASFV isolates. (e) Modulation of SLA-I expression in porcine cells infected with EP153R-deletion mutants. Cultures of IPAM cells were infected with the parental viruses E70 or its corresponding recombinant (ED4) lacking the EP153R gene. Cells collected at 40 hpi were incubated with porcine SLA-I antibodies (BL6H4, 4B7/8 or JM1E3) to analyze the expression of class I antigens (mean  $\pm$  S.D. in duplicate samples) in the plasma membrane by flow cytometry, and the mRNA transcription specific for p72 and EP153R genes by RT-PCR (f).

Figure 1 consists of five panels (b-e) illustrating the structural analysis of the H1-TM domain. Panel (b) shows a surface representation of the H1-TM domain, with helices H1, H2, and H3, and loops E1, E2, E4, E5, and E6. Panel (c) shows a ribbon diagram of the H1-TM domain, with helices H1, H2, and H3, and loops E1, E2, E4, E5, and E6. Panel (d) shows a comparison of the H1-TM domain with the CD69, EP153R, CD94, and Ly49A domains. Panel (e) shows a surface representation of the H1-TM domain, with helices H1, H2, and H3, and loops E1, E2, E4, E5, and E6, highlighting the polar and hydrophobic regions.

## Figure 1



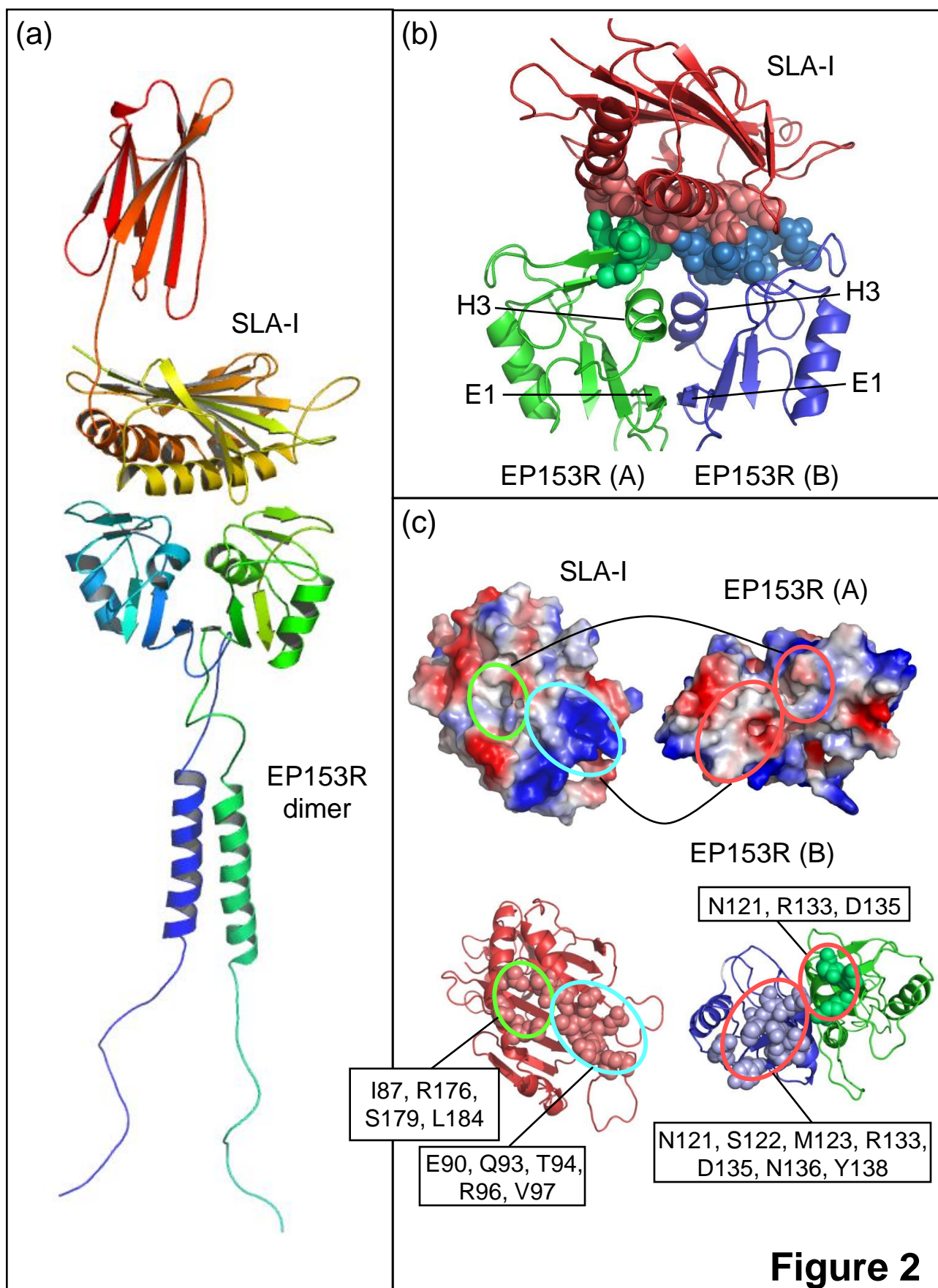


**Figure 2**



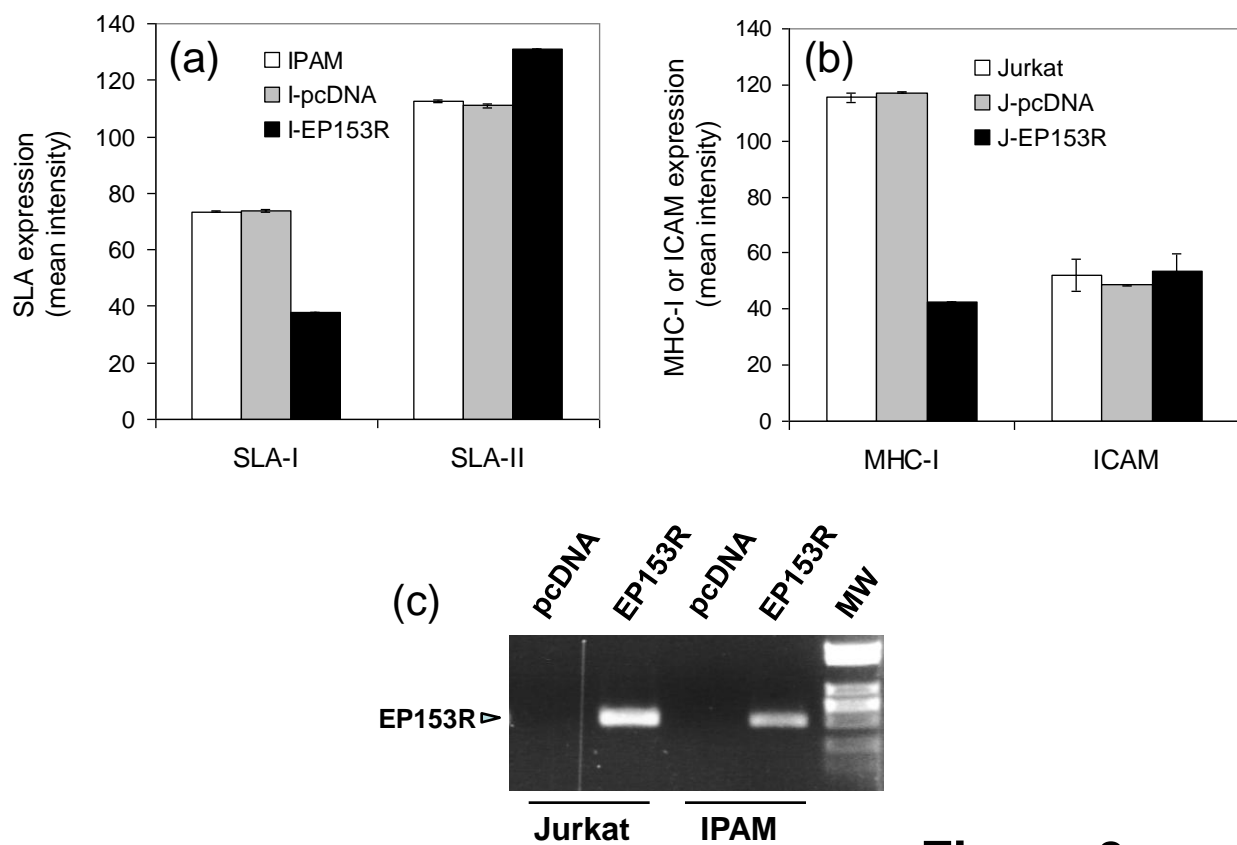


**Figure 3**

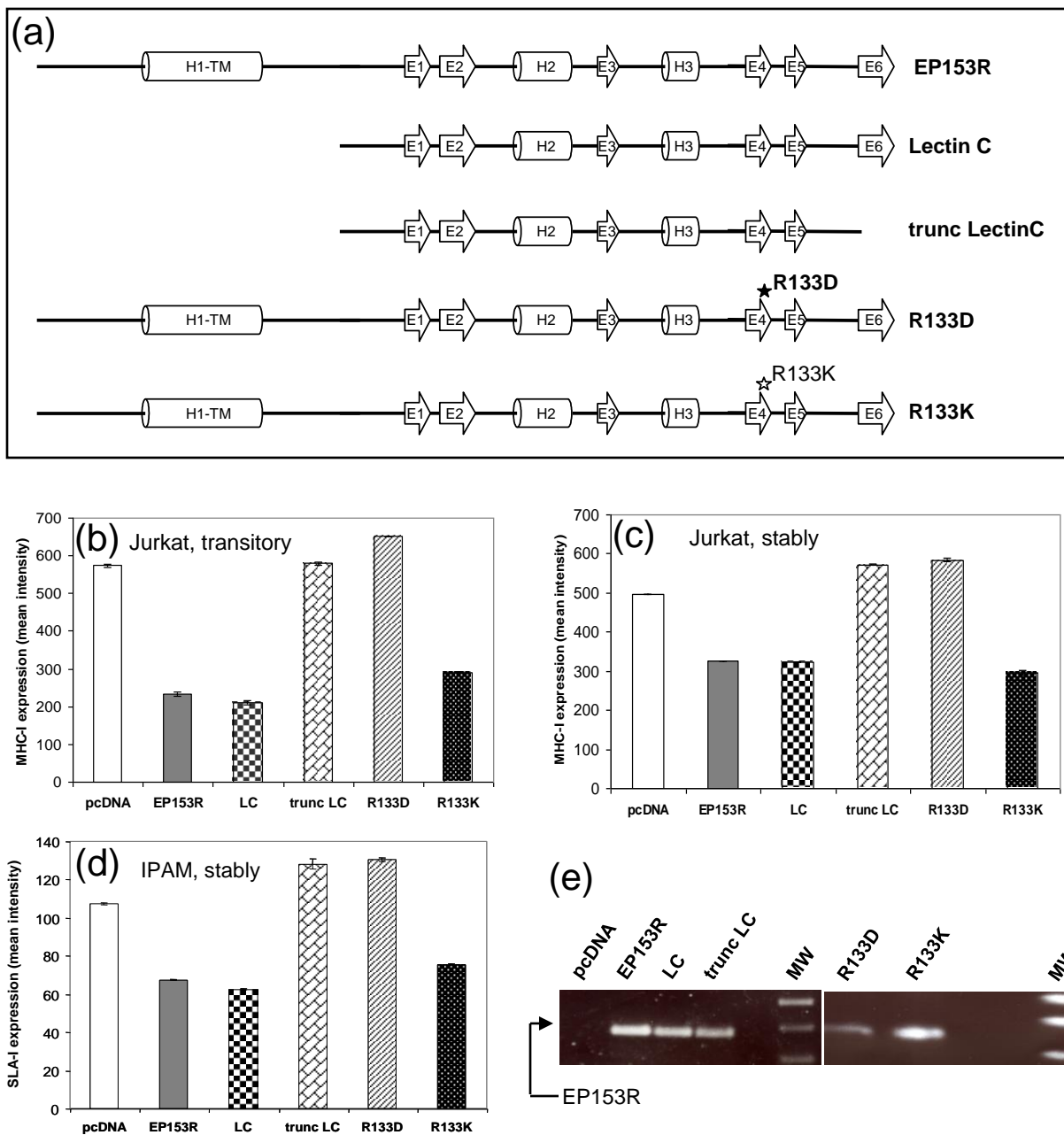


**Figure 4**

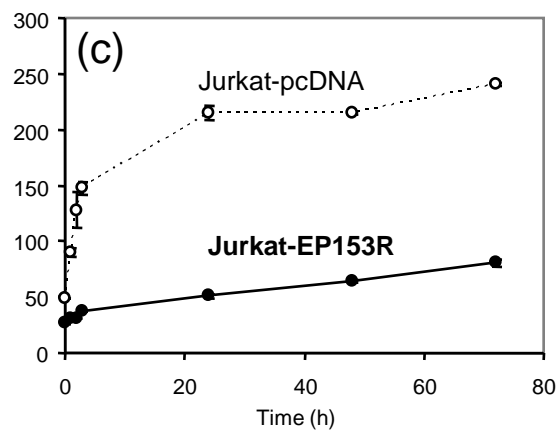
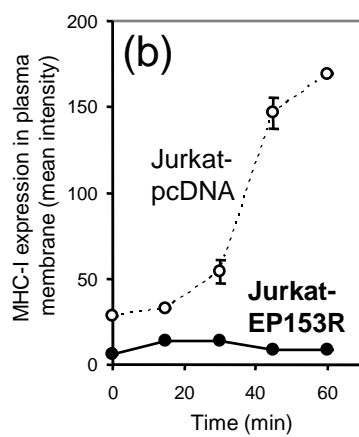
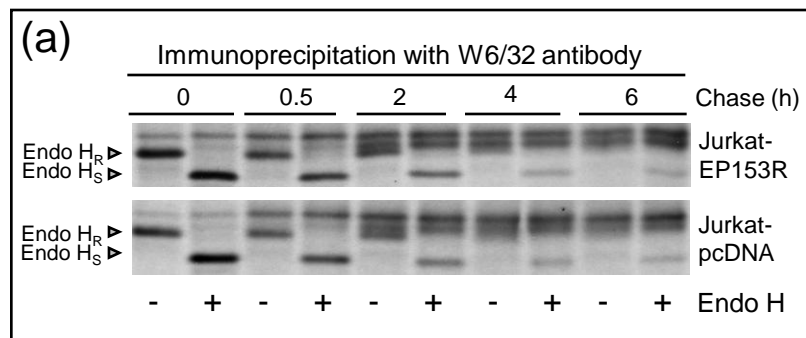


**Figure 5**

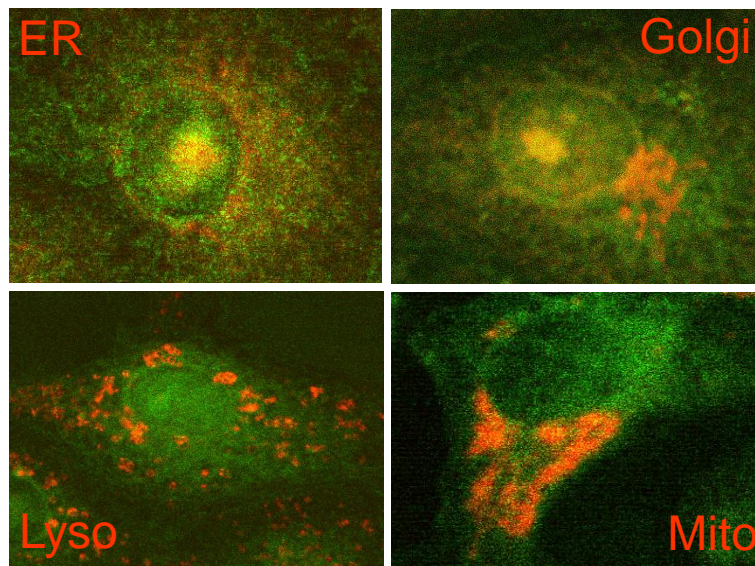


**Figure 6**

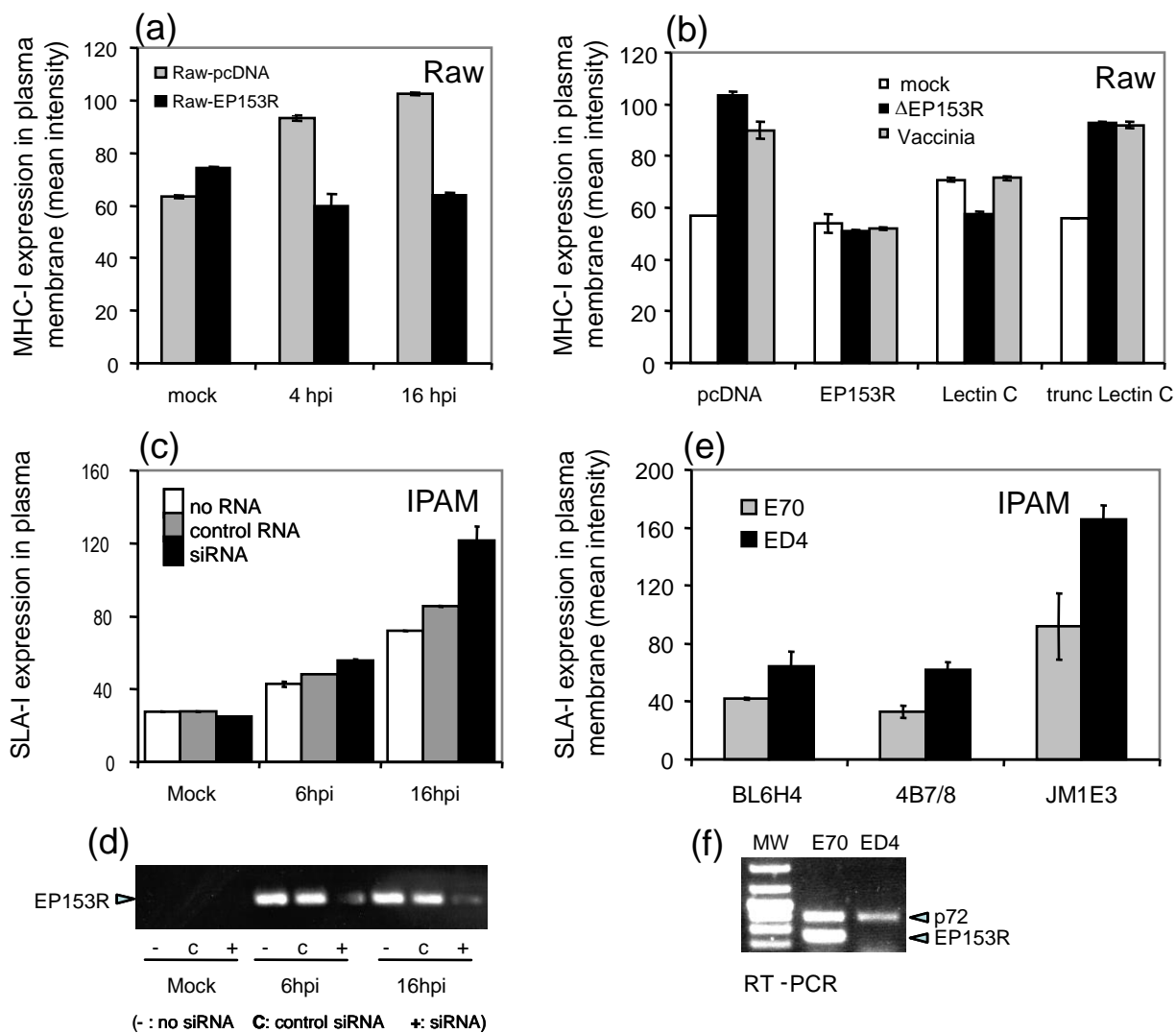


**Figure 7**